Fabrication of Molybdenum (IV) Sulfide – Zeolitic Imidazole Framework-8 (MoS_2 – ZIF-8) Membranes Supported onto Alumina Substrates for Dye Treatment in Wastewater

Siti Mastura binti Abdul Rahman, Nor Hazelah binti Kasmuri and Dr. Nur Hidayati binti Othman,

Faculty of Chemical Engineering, Universiti Teknologi Mara

***Abstract*— In order for treatment of dye content in wastewater the research was studied using a composite membrane which are known to be promising platform for textile industries. Instead of using conventional technology, membrane can withstand highly reactive solutions at various operating conditions. Composite membrane used with the combination of Molybdenum (IV) Sulfide and Zeolitic Imidazole Framework-8 (MoS_2 – ZIF-8) was prepared using simple vacuum filtration technique. This membrane prepared undergoes membrane filtration test to observed dye rejection ability and its water flux characteristics. The concentration of methylene blue dye inlet and outlet was observed throughout the test. Two parameters observed which are contact time, pressure and concentration. Concentration of dye were varied for 10 mg/L, 20 mg/L and 30 mg/L. Compare for all three concentration, 30 mg/L of dye concentration seems produced highest efficiency of dye removal. This can be concluded that the higher the concentration the higher the efficiency of dye removal. Besides, the contact time were carried out for1 hour and permeates sample collected for every 10 minutes. This study of membrane filtration was done by using three different pressure which are 0.5 bar, 1.0 bar and 1.5 bar. The optimum pressure was observed at 0.5 bar for all concentration since this helps to increase the contact time of dye solution inlet pass through membrane by decrease the flowrate of sample.**

Keywords*— MoS_2 -ZIF-8 membrane, methylene blue dye, adsorbent testing, ceramic membrane

I. INTRODUCTION

Dye is commonly used worldwide as the main components to generate colour. Basically, most industries such as textile, paper and pulp mills, dye manufacturing industries, food companies and also electroplating factories apply dye as the main composition in order to get complete process production of products [1]. Paint is one of the products produce from dyes and pigments extraction. Generally, pigments are coloured, colourless or fluorescent whether organic or inorganic insoluble in application. While dyes are actually coloured substances which soluble or undergoes adsorption process into the solution during the application. Dyes also can be classified into two types such as synthetic dyes and natural dyes. Synthetic dyes commonly based on petroleum compound while natural dyes are obtained from natural sources like plant, animal and also mineral matters [2].

Dyes produce from industrial waste usually may cause harm to health and also environment. However, there is no any proof yet regarding most of dye present in textile dyeing risk to human health at high level exposure of the workers especially in the factories. But with long-term exposure, it can be likely hazards to health performance and this chemicals presence then should be treated correctly. The most common hazards regarding the presence of reactive dye is respiratory problems which is due to the inhalation od dye particles disperse in the air. Extreme case might cause impact for the immune system. Moreover, dye also give negative impacts towards environment which it capable of altering physical or chemical properties which consequently causing harm to flora and fauna in the environment. This phenomenon was observed on the toxic nature of dyes which causes deaths of soil microorganisms and affect agricultural productivity [3].

Conventionally treated by using adsorption of activated carbon. This method used was being improvised since the conventional method cannot measure some parameter that are needed and it also can only apply at a certain limit condition. There are a few problems face when using the conventional technology. One of the problems is dye treatment were difficult to treat conventionally since when it was varied with the feed concentration and used continuously, it can be swell and cannot achieve constant performance. Other than that, it cannot operate with the presence of high reactive compounds whether in acidic or alkaline conditions and also when there is a presence of a solvents the efficiency of the operating system will be decreased. Moreover, this conventional technology also failed to operate at high operation temperature [4].

In order to produce for high efficiency of dye treatment, membrane is the most famous way which is commonly used instead of another method since this method exhibited the most excellent ability in separation especially for some materials in nanosized instead of using free settling and centrifugation. The use of membranes to filter raw water or pre-treated water is such a barrier because both microfiltration and ultrafiltration (MF/UF) have a defined pore size proven the effectiveness in reducing such contaminants in order to produce water at the safe levels.

Currently many techniques used for dye removal which involved chemically, physically and biologically. Some of the examples of current method for dye removal involved membrane filtration, coagulation and flocculation process., ion exchange process, adsorption using activated carbon, reverse osmosis and also ozone treatment. Conventionally treated by using adsorption of activated carbon commonly used as a method to remove dyes content in

wastewater. Since the conventional method cannot measure some parameter that are needed and it also can only apply at a certain limit condition. There are a few problems face when using the conventional technology. One of the problems is dye was difficult to treat conventionally since when it was varied with the feed concentration and used continuously, it can be swell and cannot achieve constant performance. Other than that, it cannot operate with the presence of high reactive compounds whether in acidic or alkaline conditions and also when there is a presence of a solvents the efficiency of the operating system will be decreased. Some study gives approaches in order to solve this problem and remove all dyes content efficiently.

However, different conditions and strategies used may affect the adsorption performance of graphene. In order to prevent decreasing of adsorption performance, the problems were being improved by combination of graphene-based materials with Zeolitic Imidazolate Frameworks (ZIFs). This this combination provided a long operating lifetime. ZIFs is a class of nanoporous solids consists of metal Zn and Co linked by imidazolate ligands [5]. In this research study, the Molybdenum (IV) Sulfide (MOS_2) was combined with Zeolitic Imidazole Framework-8 (ZIF-8) acts as membrane for the wastewater treatment. The MOS_2 – ZIF-8 membranes were synthesis using simple vacuum filtration technique. The composition of ZIF-8 was produced by synthesized the components at room temperature by using suitable method and operating conditions. Meanwhile, the Molybdenum (IV) Sulfide obtained using exfoliation method which consists of two method strategies which are by using ultrasonic and ball milling assist [6]. The MOS_2 – ZIF-8 membranes were synthesized and fabricated the membranes on supported alumina substrate [7].

Ceramic that are used for dye treatment has a lot of advantages which make it more suitable used for separation of many types of molecules. This membrane has higher pressure ratings and chemical resistance. These characteristics can be more effective recovery from backwash and chemical cleaning cycles [8]. Therefore, the risk of irreversible fouling will be low. Next, most of the ceramic membrane has higher flux in order to make the system overall more cost competitive. The flux range for this type of membrane is usually at range about 170 to 297 LMH. Besides, in term of physical properties, it can operate better and withstand highly reactive compounds. This membrane is chemically inert which has high porosity and good tunable functionality. It also has high stability of mechanical and chemical with a longer membrane's lifespan[9].
This research was conducted in order to study about the combination of MOS2 and ZIF-8 membrane for dye treatment in wastewater[10]. Molybdenum (IV) Sulfide (MOS2) is a type of 2D nanomaterials which it can be produce through certain method such as by shear exfoliation [6].

In other hands, ZIF-8 membrane was used to separate dye in wastewater treatment. The combination of ZIF-8 and MOS2 help to increase the efficiency of separation process. There are several techniques developed to prepare MOF membranes which are secondary growth by depositing the seeds, pre-treatment of support by reactive seeding or organic functional groups and also contra-diffusion synthesis of membrane by separating precursors at two sides of the support. The secondary growth is conducting via rubbing, dip-coating, thermal seeding or by repeated growth.ZIF-8 show better thermal, hydrothermal and chemical stabilities and it also very promising materials for many applications such as membrane catalysis.

Instead of combination the MOS2 with other type of membranes, the ZIF-8 was choose as an ideal combination between the two membrane. By doing study, the combination of any 2D nanomaterials (MOS2) with Metal Organic Frameworks (MOFs), it exhibited the high ratio with a long operating lifetime. The longer operating lifetime helps to reduce the cost of membrane maintenance without need to frequently doing a membrane replacement. MOFs has many advantages such as rich surface chemistry, has structure versatility, and also can tuneable the pore size in nanometer regime. With all these advantages of MOFs, it will help to further broaden their potential applications by embedded it with 2D nanomaterials and their hybrid.

II. METHODOLOGY

Figure 1 shows the steps involve in this work. This work study started with the synthesized step for ZIF-8 membrane using the solution zinc nitrate together with Hmim powder. Next, the synthesized of MOS_2 membrane using exfoliation method where the most efficient volume of solution were recorded and used in the experiments study. The membrane was coated onto alumina substrates and undergo two test which are adsorbent test and membrane test with vary the concentration and contact under UV condition using UV-vis.

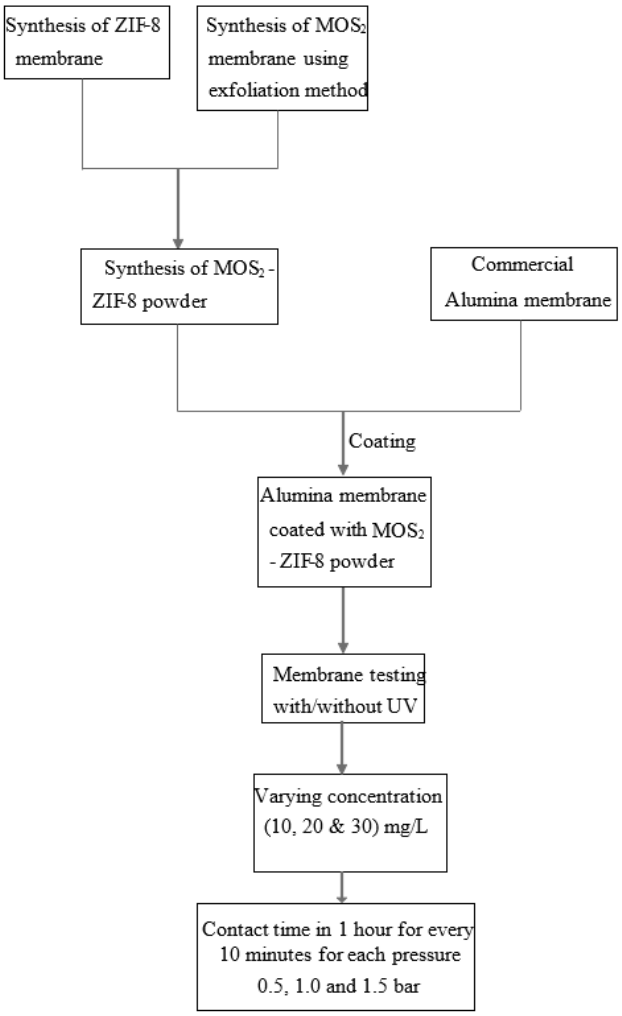

Fig. 1 shows the steps involve in this work (methodology)

A. Materials

The materials needed for preparation of ZIF-8 powder were Zn (NO3)2 6H2O (>99%, Sinopharm Chemical Reagent), 2-methylimidazole (Hmim: >99%, Alfa Aesar), CH3OH (>99%, Sinopharm Chemical Reagent). The exfoliated molybdenum (IV) sulfide (MoS_2) was prepared using MoS_2 powder (160.07 g/mol, 2 µm, 99% Aldrich) and iso propyl alcohol (60.10 g/mol, SYSTERM) as a solvent. Besides, commercial ceramic flat sheets alumina membrane with diameter of 3.3 cm was used by coating it with MoS_2 – ZIF-8 powder which this composite powder collected by dispersing method in ultrapure water as a solvent. Moreover, tap water and deionized water used as external and internal coagulants. The testing of the composite membrane was done by using methylene blue dye (99%, Merck) dissolved in distilled water[11].

B. Exfoliation of Molybdenum (IV) Sulfide Powder

The Molybdenum (IV) Sulfide membrane was prepared by exfoliation process which involved ultrasonic technique [12]. This technique involved the mixture of 100 ml pure iso propyl alcohol. The solution then added with 0.25 g of MOS2 dissolved in the solution [6].

Ultrasonic method was used for 4 hours for the mixture to undergoes ultrasonic process. When ultrasonic process completely done, the mixture was left sedimented overnight. A few layers formed after sedimented step. The ratio of sedimented formed was observed using measuring cylinder. Bottom layer of the sedimented was taken to be dried overnight in an oven at 70˚C to 80˚C. If the top layer formed in a lowest ratio, the preparation of the MOS2 can be concluded not in good range [6].

C. Synthesis of Zeolitic Imidazole Frameworks-8 powder

ZIF-8 can be produced at a room temperature condition. Two mixture were prepared before both solutions mixed together for an hour. The first solution prepared was the combination of 108.8g methanol with 4.8g zinc nitrate granules. The solution stirred and mixed evenly. Next solution prepared was involved the mixture of 108.8g methanol together with 10.6g H_{mim}.

The first and second mixture prepared were being combined using magnetic stirrer for an hour at medium speed. Make sure the mixture was covered with parafilm to avoid any contaminants substances exerted into the solution. Consequently, the contaminants exerted may affect the result and some error may occur in order to produce high purity of ZIF-8 powder. After the mixing process completely done, the mixture was poured equally into the sample tube and undergo centrifuging process for 5 minutes at 6000rpm speed. The supernatant or known as mother liquor produced from the first centrifuged process was used in order to increase the production yield of ZIF- 8 powder. Precipitate which consists of ZIF-8 produced at the bottom were rinse twice using methanol and centrifuged at same condition which is at 6000rpm speed for 5 minutes.

ZIF-8 precipitated suspended at the bottom then collected and being dried in an oven overnight at a range temperature 60˚C to 70˚C. Dried ZIF-8 then was crushed using mortar until it become ZIF-8 powder. The production yield produced then being weighted using weighing balance. If it is necessary to increase the yield, synthesis ZIF- 8 repeatedly using the same step but using mother liquor produced in the first synthesis process as the solvent instead of using pure methanol. [13]. Figure 2 below described the steps involved in synthesized the ZIF-8.

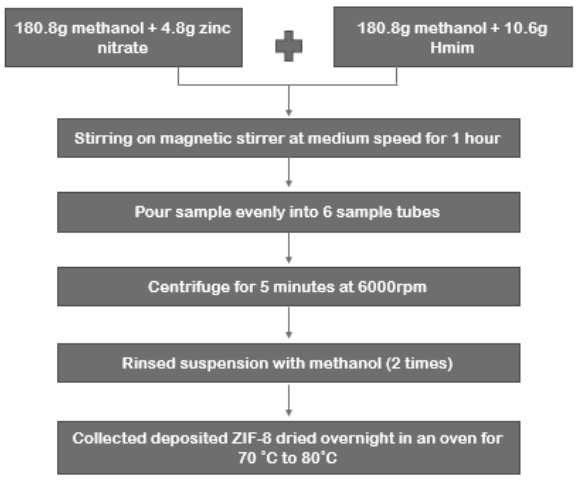

Fig. 2 Steps used in order for synthesized of ZIF-8 powder

D. In-Situ Synthesis of MoS_2 – ZIF-8 solution onto Alumina Flat Sheet Membrane

The MOS2 seeds produced after undergo exfoliation process while ZIF-8 produced at a room conditions temperature after being mixed. Both of these seeds were combined together in order to improvised the present of conventional membrane resulted for new improvised membrane which can increase the filtration efficiency. The combination of these membranes completely done by simple vacuum filtration techniques, using the vacuum filter holder with the fritted glass support. The most effective composition of MOS2 to ZIF-8 was chosen for 50% ZIF-8/50% MoS_2. The 0.1 g exfoliated MOS2 powder and 0.1 g ZIF-8 powder were dispersed in 100ml ultrapure water solution and undergo sonicating process for about 1 hour and followed by the vacuum filtering of the diluted solution over the alumina support in order to get pure membranes. [14]. Coating step was done by coating the membrane for 60ml prepared solution using vacuum filtration technique. Figure 3 illustrated the set-up apparatus involved for in-situ synthesis of MoS_2 – ZIF-8 membrane using simple vacuum filtration technique.

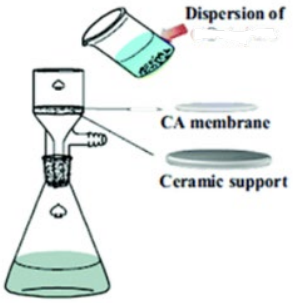

Fig. 3 Set-up apparatus for in-situ synthesis of MoS_2 – ZIF-8 membrane using simple vacuum filtration technique.

E. Pure water flux

Pure water flux is the test to measure the permeate flow volume passed through the membrane. This test was conducted in a lab scale which involved dead-end mode and cross-flow mode. First of all, the membrane is compacted under six bars of ultrapure water until it reached the equilibrium state. Usually, this test was conducted for 1 hour where the permeate volume was taken for every 10 minutes interval. The fluxes are calculated using the following equation[15];

$$J = \frac{V}{A\Delta t} \quad \text{(Eq. 1)}$$

J = Pure water flux (L/m^{2}h)
V = Volume of permeated pure water (L)
A = Area (m^2)
t = Time (h)

F. Dye Rejection

This method was recorded by measuring the concentration of permeate water using UV-vis. Set up apparatus used for dye rejection step was shown in Figure 4 [16]. The sample water was added into feed water tank and the initial concentration of dye solution recorded before being treated using coated membrane. Permeates sample were collected every 10 minutes for 1 hour. Record the final volume and concentration in order for next step of dye rejection calculation.

$$R\ (\%) = \left(1 - \frac{C_p}{C_f}\right) \times 100\% \quad \text{(Eq. 2)}$$

R = Rejection rate (%)
C_p = Concentration of permeate
C_f = Concentration of feed

G.Membrane Testing

Many factors should be considered in order to choose the suitable membrane used which were included the concentration of dye used, contact time of the process and also the pressure exert on the membrane. The major factors studied were based on the concentration and the contact time. Membrane used in this study involved the combination of MoS_2 and ZIF-8. The most applicable concentration, contact time and pressure were recorded based on its efficiency and used as an operating condition to run the system used as Figure 4. The method on how to selected the most suitable conditions for the membrane is stated below;

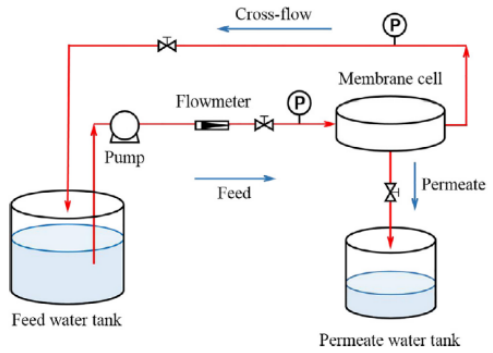

Fig. 4 Membrane filtration crossflow unit set-up apparatus used for membrane testing [14]

Membrane testing was done based on the samples concentration which was varied for 10 mg/L, 20 mg/L and 30 mg/L. The effect of concentration was characterized in order to obtained the optimize concentration of dye used. This is important since the membrane is very sensitive to the dye content which unexpectedly will be lower the efficiency of membrane and its life span. The experiment was conduct in 1 hours for each concentration. The volume of the sample recorded for every 10 minutes contact time. The samples for each concentration was run in 1 hour for each pressure varied for 0.5 bar, 1.0 bar and 1.5 bar. The effect of the pressure was observed based on the flow of the sample through the membrane which effect the quantity of permeate water [17].

III. RESULTS AND DISCUSSION

A. Characterization of synthesized powder

The characterization involved ZIF-8 powder, exfoliated MoS_2 powder, pure MoS_2 powder and MoS_2 – ZIF-8 powder. The characterization can be classified into two major categories which are chemical stability and thermal stability performances. Some of the characterization equipment involve for chemical stability were X-Ray Diffraction (XRD) (X'Pert PRO model) and Fourier Transform Infrared Spectra (FT-IR) were observed using a Bruker Vertex 70 FT-IR spectrometer which equipped with a Ge-coated KBr beam splitter while Thermal Gravimetric Analysis (TGA) was used to monitor the thermal stability of the synthesized powder. Below shows the result for the sample powder characterizations;

1. Crystallization structures of synthesized powder

XRD analysis was carried out to identify the crystal structure of ZIF-8, Exfoliated MoS_2 in propanol, pure MoS_2, Exfoliated MoS_2 in isopropanol and also composite powder MoS_2 – ZIF-8 as shown in Figure 5 below.

From the graph below it can be observed that all XRD peaks were sharp and well defined with slight peak. This can be suggested that the ZIF-8 particles were fully crystalline in nanometer range. Regarding the literature data, the ZIF-8 particles exhibit sharp diffraction angle (2θ) at 7.319˚, 10.311˚, 12.674˚, 14.697˚, 17.995˚ and etc. which is totally matched. There is no also additional peaks which unrelated to ZIF-8 crystallographic data which means it can be concluded that the reaction product produced could be confirmed as a pure phase ZIF-8 with no impurity[18]. XRD patterns also indicated that no polymorphism or additional surface growth occurred during the synthesized process. Hence the presence of impurity like water and methanol can be neglected[19].

Meanwhile, the peak of the MoS_2 can be observed at diffraction angle (2θ) at 14.357˚, 32.6˚, 39.5˚ and etc. All the diffraction peaks of the two samples can be indexed to the hexagonal MoS_2[20]

Furthermore, synthesized of composite powder MoS_2 – ZIF-8 resulted by formation of peak where likely same with MoS_2 but more crystalline peaks structure formed since there is presence of zeolitic imidazole frameworks in the composite powder. By referring to the graph in Figure 5, the maximum peak was at 14.357˚ exactly same with the maximum peak of MoS_2 but this composite powder produced more sharper peak of crystalline structure. This crystalline structure formed well defined by the mixture of two major components which are MoS_2 powder and ZIF-8 powder where can be observed through the peaks of particles in range of targeting final composite powder.

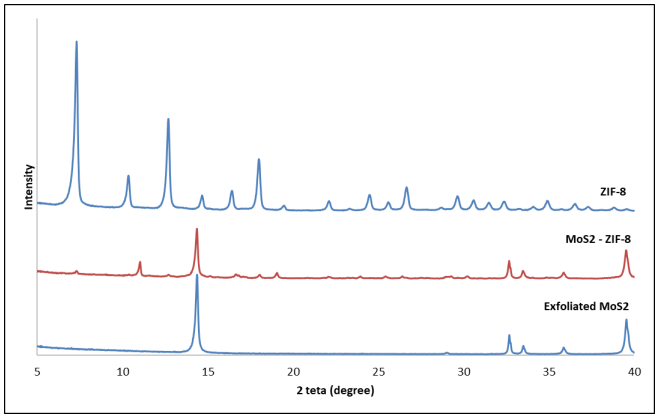

Fig. 5 XRD spectrum for ZIF-8, Exfoliated MoS_2 in propanol, Exfoliated MoS_2 in isopropanol, pure MoS_2 and also composite powder MoS_2 – ZIF-8

2. Analysing the functional group of synthesized powder

The graph below shows the result for the three type of samples which are ZIF-8 powder, exfoliated MoS_2 powder and MoS_2 - ZIF-8 powder. Fourier Transform Infrared Spectra (FTIR) of model Spectrum One by Perkin Elmer was used in order to identify the functional group of a samples. The framework structure for both exfoliated MoS_2 and ZIF-8 particles were performed over the wavenumber range 4000 cm^{-1} to 500 cm^{-1} at a resolution of 4 cm^{-1} [18].

Based on the figure 6 below, all the characteristic peaks corresponding to imidazole structure of ZIF-8 were present. This included the peak at 3690 cm^{-1} (aromatic C-H stretching vibration), at peak 2879 cm^{-1} (aliphatic C-H stretching vibration) and at 1413 cm^{-1} shows (C=N stretching vibration). Besides, 3 individual peaks were found at 1146 cm^{-1}, 996 cm^{-1} and 759 cm^{-1} where all of its which are associated with C-N stretching vibrations. Others peaks appeared correspond to the in-plane, out-plane and also associated with stretching of the bending of imidazole ring [18].

Meanwhile, characterization of MoS_2 using FTIR shows a few absorption peaks which can attributed to MoS_2 nanosheets layer [21]. The peaks of exfoliated MoS_2 characteristics were shown at peak 1097 cm^{-1}, 613 cm^{-1} and at 468 cm^{-1} where they are associated with the C-N bonds vibrations that subsequently cause the formation of nanosheets layer [22].

Moreover, graph in Figure 6 also illustrates all the crystalline structure of composite powder MoS_2 – ZIF-8 where it can clearly show that all the structure corresponding to the imidazole structure together with nanosheets layers structure presented. This contributes to increase the crystalline structure presented compare to pure ZIF-

8 particles and exfoliated MoS_2. The existing crystalline particles can be observed using the peaks presented of composite powder. The aromatic C-H stretching vibration bond can be obtained at peak 2970 cm^{-1} while at 1739 cm^{-1} shows C=N stretching vibration. Besides, other 4 individual peaks at 1374 cm^{-1}, 1217 cm^{-1}, 1146 cm^{-1} and 747 cm^{-1} present C-N stretching vibration bond obtained from the composite powder MoS_2 – ZIF-8.

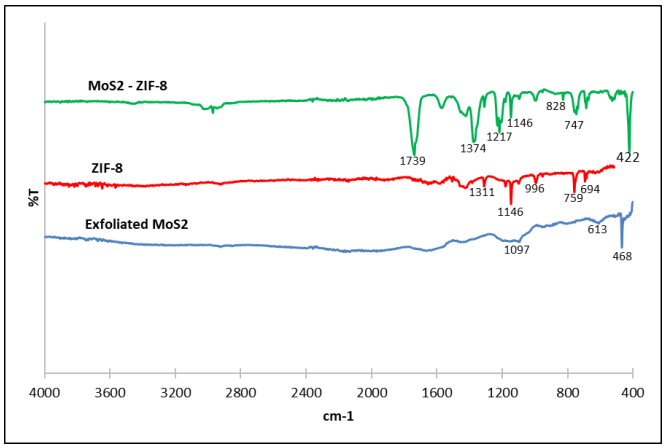

Fig. 6 FTIR spectra of ZIF-8, exfoliated MoS_2 and MoS_2 – ZIF-8 particles using the same wavenumber range from 4000 cm^{-1} to 500 cm^{-1}

3. Thermal stability performances of synthesized powder

Figure 7 illustrates the resistance of materials (ZIF-8 powder, MoS_2 powder and MoS_2 - ZIF-8 powder) towards thermal. The properties of thermal resistance were studied using Thermogravimetric Analysis (TGA). The process then continues by supplying the nitrogen gas at room temperature. The temperature started at 25˚C to 1000 ˚C which at 10 ˚C/min heating rate. Figure 7 shows the result of the weight loss of pure MoS_2 powder and exfoliated MoS_2 powder. Meanwhile, Figure 8 shows the weight loss of ZIF-8 powder against heating temperature.

From the figure 7 (a) below we can observe that for the first 650˚C temperature (200˚C to 850˚C) exfoliated MoS_2 inhibits higher weight loss compare to pure MoS_2. Pure MoS_2 powder was used as a reference with a great thermal stability characteristic. As we can see, there are two TGA region curve for both pure MoS_2 and exfoliated MoS_2. Where the first 600˚C (229.21˚C to 829.21˚C) shows the slightly weight loss from 100% to 99.2% (pure MoS_2) and 100% to 99.4% (exfoliated MoS_2) where it is corresponds to the moisture absorption in MoS_2 powder but decomposition of MoS_2 takes place starting from 829.21˚C to 1029.21˚C[23].

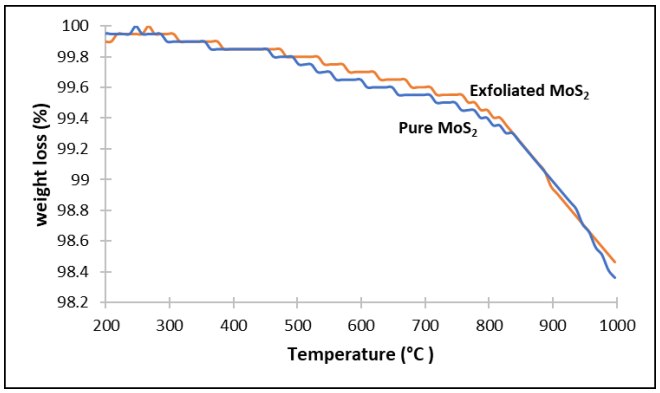

Fig. 7 TGA analysis of pure MoS_2 and exfoliated MoS_2

Besides, from the other Figure 8 which is shows the characterization of ZIF-8 particles. There are two TGA regions in curve in Figure 8 which shows the specific process of absorption and decomposition. For the first 600˚C shows that the weight is slightly loss from 100% to 90% which is due to moisture adsorption process on the sample[18]. Then, starting from 600˚C to 1000˚C the decomposition of ZIF-8 powder takes place where it is indicating of phase transformation of organic frameworks of ZIF-8 particles [24].

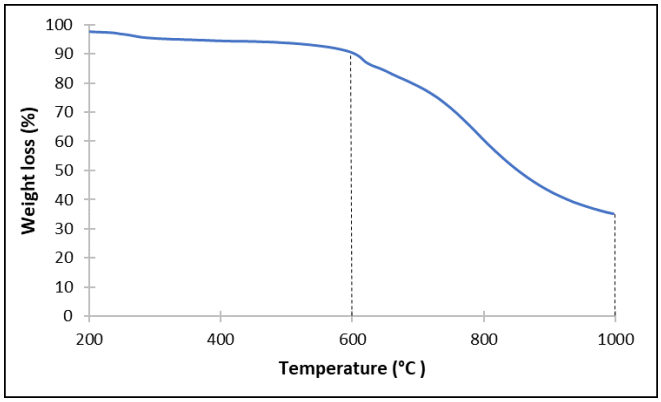

Fig. 8 TGA analysis of ZIF-8

B. Characterization of fabricated membrane

The characterization involved bare alumina membrane and alumina membrane coated with MoS_2 – ZIF-8. The characterization was done in order to study the morphological of membrane including the pore size, roughness, porosity and surface condition of membranes. This morphological study of the membrane can be observed using Mercury Porosimetry, Digital Microscope, Atomic Force Analysis (AFM) XE-100, Field Emission Scanning Electron Microscope (FESEM Nanosem 430, 10eV) and Scanning Electron Microscopy (SEM) (Hitachi S-4800). While, the hydrophilicity of the membrane can be observed using contact angle (AST products model VCA3000S). Below shows the result for the sample membrane characterizations;

1. Surface morphology and pore size of bare alumina membrane and membrane coated with MoS_2 – ZIF-8

Mercury porosimetry analysis were done for two sample which are bare alumina membrane and alumina membrane coated with MoS_2 – ZIF-8. The pore size distribution can be determine using this type of equipment. The mean pore size of bare alumina was 89.33µm (Figure 9). But after the membrane undergoes the coating process using MoS_2 – ZIF-8 powder, the mean pore size decreases to 6.03 µm (Figure 10). It is show that the pore size of the membrane become smaller after the coating process. This peaks of the coated alumina membrane obviously illustrated that the pores in the membrane partially filled or coated with the substrates used (MoS_2 – ZIF-8 powder)[25]. Figure 8 below illustrated the results for both bare alumina membrane and alumina membrane coated with MoS_2 – ZIF-8 solution after undergo mercury porosimetry characterization process. The graph was draw between the intrusion pore size versus it pore diameter.

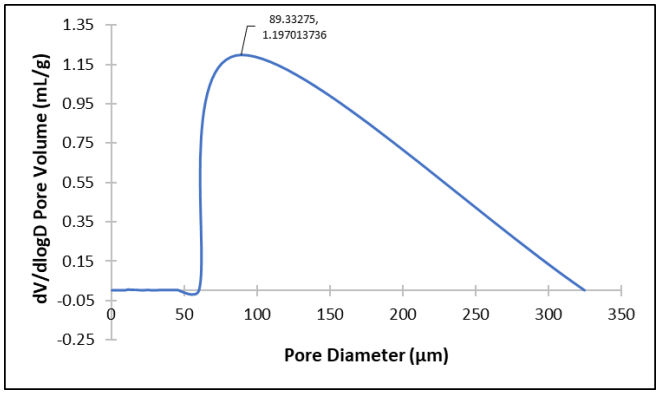

Fig. 9 Shows the graph of log differential intrusion (mL/g) of bare alumina versus the pore diameter (µm) by using mercury porosimetry

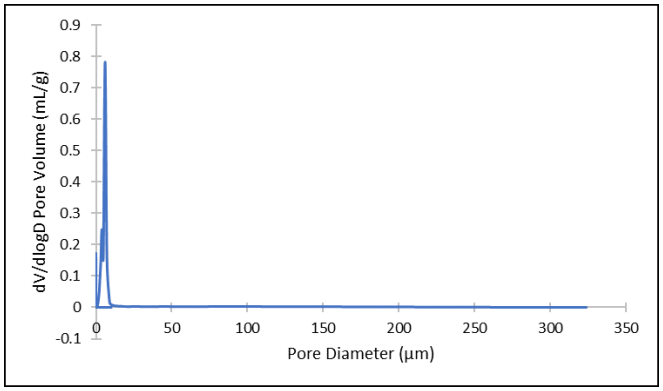

(i) alumina membrane coated with MoS_2 – ZIF-8 pore diameter ranges from 0 µm to 325 µm

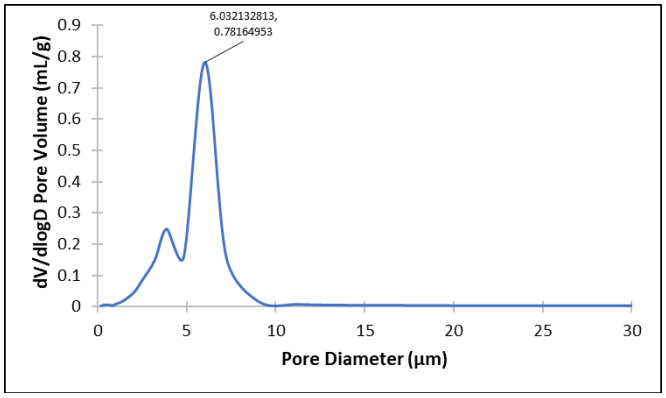

(ii) zoom in diagram of alumina membrane coated with MoS_2 – ZIF-8 for pore diameter range from 0 µm to 30 µm

Fig. 10 Shows the graph of log differential intrusion (mL/g) of alumina membrane coated with MoS_2 – ZIF-8 versus the pore diameter (µm) by using mercury porosimetry

Other than that, surface condition of the membrane was observed using three different equipment based on its functionality and ability of magnification. The 2-D and 3-D surface of both bare and coated membrane was characterized using Atomic Force Microscopy (AFM) shown in Figure 11. From the characterization procedure using AFM it can be concluded the surface roughness of the membrane by comparing the root mean squared roughness (Rq) of bare membrane with coated MoS_2 – ZIF-8 membrane which show that the coated membrane has much more rougher surface compared to bare membrane where the surface roughness was 1036 nm while bare membrane was 286.497 nm stated in Table 1 below. This roughness was an indicator to show the changes in surface morphology upon to the growth of MoS_2 – ZIF-8 composite nanostructures on the alumina membrane. Increasing value of root mean squared roughness showed the increasing amount of nanostructure onto the membrane [26].

Table 1: Roughness of the membrane using AFM

Sample membrane	Root mean squared roughness (Rq), nm
Bare alumina	286.497
Coated with MoS_2 – ZIF-8	1036

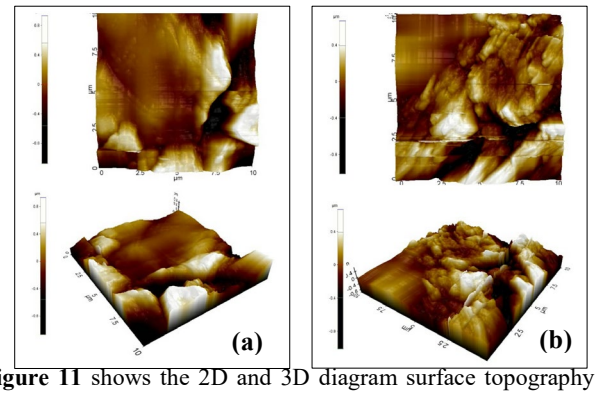

Figure 11 shows the 2D and 3D diagram surface topography **(a)** AFM image for bare alumina, **(b)** AFM image for MoS_2 -ZIF-8 coated on alumina.

The detailed surface and cross section morphology of membrane can be obtained using SEM and FE-SEM characterization equipment [27]. This equipment shows the surface roughness and morphology by using magnification of 1000, 5000 and 10000. Figure 12 shows the surface roughness of the bare membrane and coated membrane before the testing with different magnification. By using 1000 magnification the pore size seems to be at 10 µm. For 5000 and 10000 magnification show by pore size of 1 µm. Meanwhile, Figure 13 shows the morphological of coated alumina membrane using same magnification used for bare alumina membrane. This clearly show that the surface of the coated membrane rougher than bare membrane since there is a nanostructure of composite membrane growth on the surface which much more narrower passages than the original bare alumina membrane [25]. Meanwhile the bare membrane looks much more porous and larger in pore size. Uncoated membrane yielded to poor coverage on membrane filtration process. Further illustrations on surface morphological can be observed referring to figure below;

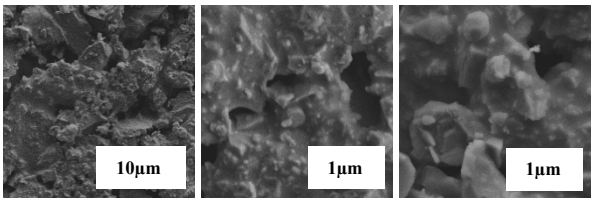

Figure 12 Bare membrane morphological surface structure

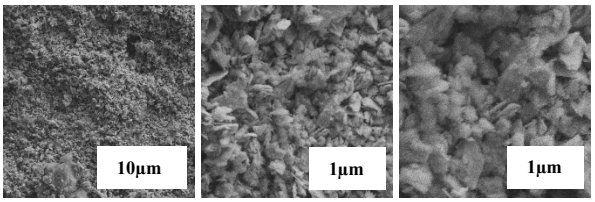

Figure 13 Membrane coated with MoS_2 – ZIF-8 morphological surface structure

Meanwhile Figure 14 (i) and (ii) show the surface morphological and cross section after undergoes dye treatment process. The surface seems contaminated with methylene blue dye particles on its surface which can be seen by a few dark spots that was circled in Figure 14 (i).

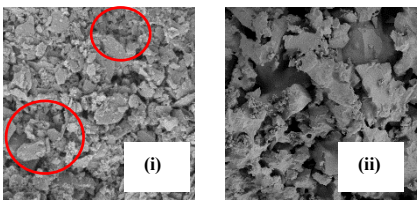

Figure 14 shows the morphological surface roughness and cross section study of coated membrane after undergo dye treatment where **(i)** surface morphological and **(ii)** cross section

Moreover, the morphological of the membrane's pore size can be observed using digital microscope shown in Figure 12 the topography diagram for cross section area of alumina membrane. Figure 15 (a) illustrated that the bare alumina membrane after undergo water flux process using deionized water. The observation shows that some contaminants which is due to the equipment scaling and contaminants was being absorb and filter by the membrane. Meanwhile, Figure 15 (b) shown the cross section of coated alumina membrane which is partially filled with the coated substrates (MoS_2 – ZIF-8 powder). The particles of the MoS_2 – ZIF-8 substrates clearly can be observed through the pore of the membrane. Finally, the bare membrane cross sectional diagram was shown as Figure 15 (c) where this bare membrane looks much clear without any coated substrates in the pore. This subsequently can decrease the membrane filtration efficiency compare to coated alumina membrane.

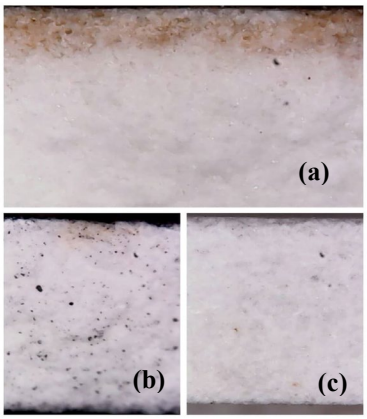

Fig. 15 Topography diagram using digital microscope **(a)** bare alumina membrane after undergo water flux process, **(b)** alumina membrane coated with MoS_2 – ZIF-8 substrates and **(c)** bare alumina membrane

2. Hydrophilicity of bare alumina membrane and membrane coated with MoS_2 – ZIF-8

Contact angle analysis was carried out to identify the hydrophilicity and its wetting strength of the membrane surface. It is carried out in the air temperature 25˚C and at pressure 1 atm. The size of the droplet chosen was 7µ. This testing conducted for two type of sample which are bare alumina membrane (Figure 17 (a)) and alumina membrane coated with MoS_2 – ZIF-8 (Figure 17 (b)). Degree between the water droplets and the membrane surface indicates the range of hydrophilicity of the membrane [28]. The degree of hydrophilicity was shown in the Figure 16 below;

Fig. 16 Degree of hydrophilicity of membrane

From Figure 17 (a) it shows the degree of bare alumina membrane is smaller than the coated alumina membrane which at 20.30˚. This show that the bare alumina membrane much more hydrophilic type of membrane which the water droplets can easily pass through the pore. Besides, the coated alumina membrane with composite particles, MoS_2 – ZIF-8 clearly show that increase the degree of hydrophilicity at 89.50˚ which the water partially can pass through the pore. This may increase the wastewater filtration efficiency which the pore of the membrane decreases after undergoing coating process. Therefore, the dye particles contaminants can easily trap between the pore of the membrane[29].

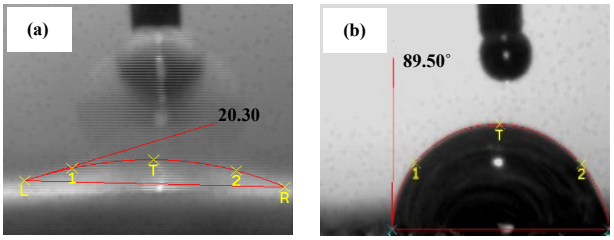

Fig. 17: Contact angle of membrane **(a)** Bare alumina membrane (0 wt%) and **(b)** Alumina membrane coated with MoS_2 -ZIF-8 (0.6 wt%

C. Membrane absorption of liquid using water flux comparison

The efficiency of adsorption of the membrane used was observed by comparing method between bare membrane and coated membrane. Surface area of membrane contact with water was 7.069 cm^2. Both membranes were run with deionized water for 1 hour and volume of sample recorded for every 10 minutes. The water flux then calculated using the volume sample collected using Equation 1. Following data calculated were tabulated as Table 2 below;

Time (min)	Type membrane	Water flux (L/m^2.h)		
		1.5 bar	1.0 bar	0.5 bar
10	Bare	3072.57	1663.6	1052.48
	Coated	2868.86	1273.16	407.41
20	Bare	2953.74	1391.99	976.09
	Coated	2665.16	1188.29	356.49
30	Bare	2588.77	1341.07	916.68
	Coated	2546.33	1154.34	322.54
40	Bare	2278.96	1188.29	882.73
	Coated	2206.82	1052.48	254.63
50	Bare	2037.06	1103.41	848.78
	Coated	0.19692	933.65	212.19
60	Bare	1837.6	1086.43	797.85
	Coated	1697.55	916.68	169.76
Average	**Bare**	2461.45	1295.8	912.44
	Coated	2325.65	1086.43	287.17

Table 2: Water flux data for bare alumina

The following Figure 18 shows the calculated water flux using bare membrane while Figure 19 shows the calculated water flux using membrane coated with MoS_2 – ZIF-8 for 1 hour for each pressure (0.5, 1.0 and 1.5 bar).

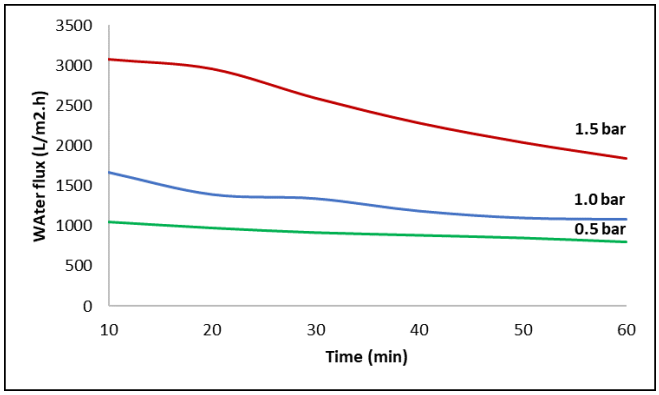

Figure 18: Water flux using bare alumina membrane

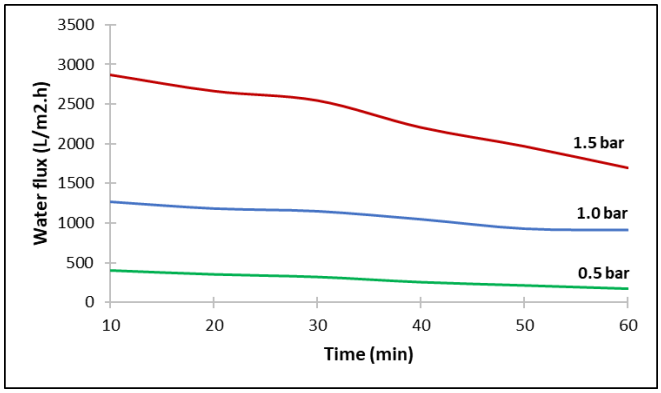

Figure 19: Water flux using membrane coated with MoS_2 – ZIF-8

From both Figure 18 and Figure 19 it can be observed that by using coated membrane the water flux can be reduced since the pore size of the membrane seen become more smaller compare to bare membrane. This also reduce the water contact with the membrane's surface subsequently increase the efficiency of membrane filtration[15]. The water flux at 1.5 bar for bare alumina membrane looks much higher compare to coated membrane which is at 2461.45 $L/m^2.h$ water flux where coated alumina was slightly low at 2325.65 L/m^2h.

Furthermore, the water flux of the membrane can be observed slightly decrease with decreasing of pressure exert through the process. The pressure helps in order to increase the water flowrate. As the water flowrate increase the water flux also increase since water flowrate is directly proportional to water flux. But, in order to has high efficiency of membrane filtration, the lower pressure, 0.5 bar was the suitable parameter should be used as it can increased the contact time of the water particles onto the surface of membrane so that the water can be treated efficiently.

D.Dye rejection

After membrane filtration process, all the sample collected were undergo UV-vis test (UV-visible Perkin Elmer Lambda 750) in order to determine the final concentration of dye solution after being treated with coated MoS_2 – ZIF-8 membrane. The data for the concentration of the solution can be extracted using the calibration curve of the dye solution graph. In order to complete the calibration curve data, the dye solutions were prepared for 5ppm, 10ppm, 15ppm, 20ppm, 25ppm and 30ppm then run for UV-vis testing by using 665nm wavelength. The standard calibration curve for dye solution was increase linearly with correlation coefficient (R^2) value of 0.9806. Graph in Figure 20 shows the standard calibration curve for methylene dye solution at 665nm wavelength.

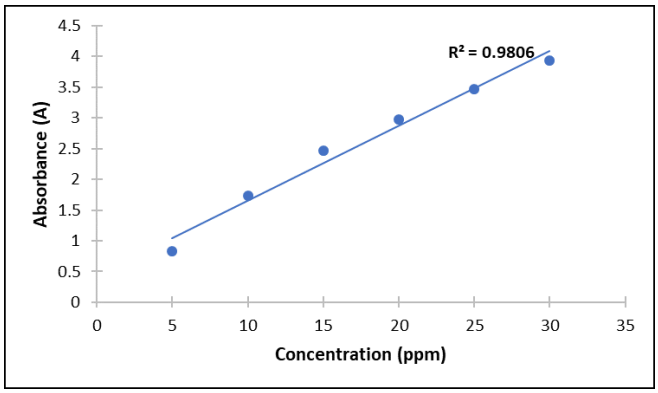

Figure 20: Standard calibration curve for methylene blue solution using UV-vis at 665nm wavelength

From the standard calibration curve, the sample permeates dye solutions were tested to determine the final concentration before being calculated using Equation 2 to find the dye rejection of the sample. The average final concentration and average dye rejection after being extract from the above data can be summarized as below Table 3.

Initial conc. (ppm)	Final concentration (ppm)			Dye rejection (R%)		
	0.5 bar	1 bar	1.5 bar	0.5 bar	1 bar	1.5 bar
10	6.093	7.014	7.792	39.068	29.861	22.076
20	13.846	13.336	13.096	30.768	33.319	34.519
30	14.36	15.391	19.224	52.132	48.698	35.920

Table 3: Average final concentration and average dye rejection extracted from standard calibration curve

From the above data it shows that dye rejection was highest at 30 ppm concentration of dye solution by using 0.5 bar pressure for the process which is for 52.13% dye rejection occurs. The lower the pressure used, the slower the flowrate of dye solution pass through the membrane. Hence, this increase the contact time between the solution and the membrane surface. In order to increase the efficiency of the membrane filtration, the flowrate was one of the important factors that should be considered as it can be controlled by lower the pressure used. If the pressure used was high, the solution enters the membrane can possibly cannot be treated well hence the efficiency of filtration decrease. Below shows graph based on data collected from Table 3. The illustration of the tabulate data was shown in Figure 21.

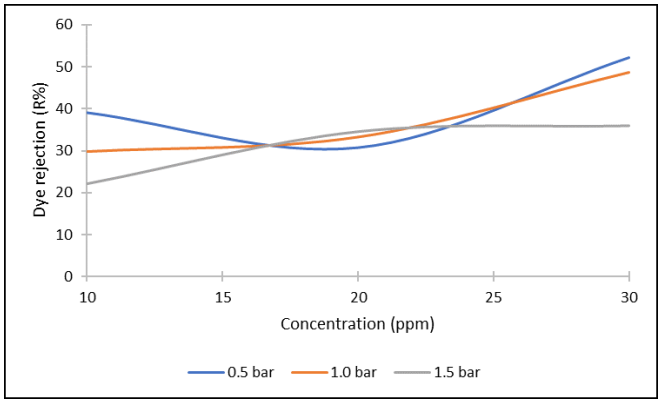

Figure 21: Dye rejection of permeates water

From the following dye rejection data, it can be observed that the dye solution sample partially treated since the highest dye rejection only for 52%. This show that half of the dye contaminants in the solution were not treated. This can be concluded that based on two factors which are type of membrane used and also type of materials to be treated. This research can be improved by change the membrane used. Instead of using commercial ceramic membrane it can be replace by using polymeric ceramic membrane. This is because of the pore size of the polymeric membrane was smaller compare to ceramic membrane. This membrane's pore size was suitable for dye treatment since dye consists of very small particles molecules. Besides, by using polymeric membrane it can control fouling effect of membrane since methylene blue dye can cause colloidal fouling layer. Membrane fouling was one of the expected effect since dyes can be accumulated on the surface of the membrane [30]. In other hand, the ceramic can consistently use in this research but for different type of removal substances which much larger in particles size. One of examples of substance could be oily water contaminate solution treated with ceramic membrane coated with MoS_2 – ZIF-8. This particle of oily water should be much suitable to treated using ceramic since ceramic membrane consists of larger

particles compare to polymeric membrane. Although the sample dye solution not fully recovered using coated membrane but, this research show some of dye particles partially treated resulted by reducing the sample permeates solution after the membrane filtration testing.

IV. Conclusion

The membrane of alumina coated with MoS_2 – ZIF-8 clearly show can increases the efficiency of dye removal in wastewater. It also concluded that the synthesized of the particles ZIF-8 and MoS_2 was successfully done as it was obeyed the physical and chemical testing characterization. The in-situ step in fabricate the composite substrate MoS_2 – ZIF-8 was done using vacuum filtration method at 0.6 wt% of solution (50%/ZIF-8 + 50%/MoS_2). The removal of the dye contaminants successfully completed which achieved the objective in this research for 30 ppm concentration of sample dye at 0.5 bar operating pressure used. Although the sample dye solution partially treated, but it shows the reduction in term of concentration and slightly achieved dye rejection in small amount. This research could be improved using polymeric membrane replaced ceramic membrane as it has more suitable criteria compatible to dye particles size or oily wastewater can be used as the main substances treated using this coated membrane.

Acknowledgment

Thank you to my supervisors Dr. Nur Hidayati Othman and Mrs. Hazelah Kasmuri, Ministry of Higher Education for the financial support and Universiti Teknologi MARA (UiTM) for all the support in equipment and apparatus along my research.

References

[1] A. G. Püntener *et al.*, *Industrial Dyes (Chemistry, Properties and Applications)*. 2003.

[2] A. Gürses, M. Açıkyıldız, K. Güneş, and M. S. Gürses, "Dyes and Pigments," 2016.

[3] M. A. Hassaan and A. El Nemr, "Health and Environmental Impacts of Monsanto's Roundup Pesticide," *Org. Consum. Assoc.*, no. November, 2017.

[4] M. Zielińska, K. Bułkowska, A. Cydzik-Kwiatkowska, K. Bernat, and I. Wojnowska-Baryła, "Removal of bisphenol A (BPA) from biologically treated wastewater by microfiltration and nanofiltration," *Int. J. Environ. Sci. Technol.*, vol. 13, no. 9, pp. 2239–2248, 2016.

[5] L. Li, J. Yao, R. Chen, L. He, K. Wang, and H. Wang, "Infiltration of precursors into a porous alumina support for ZIF-8 membrane synthesis," *Microporous Mesoporous Mater.*, 2013.

[6] E. Varrla *et al.*, "Large-Scale Production of Size-Controlled MoS_2 Nanosheets by Shear Exfoliation," *Chem. Mater.*, 2015.

[7] H. W. and Y. M. L. Seungju Kim, "2D Nanosheets and Their Composite Membranes for Water, Gas, and Ion Separation Seungju," *J. Gasellschaft Dtsch. Chem.*, 2019.

[8] B. L. Wise *et al.*, "Hydraulic Cleaning Method for Ceramic Membranes – A More Conventional Approach to Facilitate Retrofits Hydraulic Cleaning Methods for UF / MF Membranes," pp. 1–14, 2015.

[9] H. Wang *et al.*, "Graphene-based materials: Fabrication, characterization and application for the decontamination of wastewater and wastegas and hydrogen storage/generation," *Adv. Colloid Interface Sci.*, 2013.

[10] H. Ting, H. Y. Chi, C. H. Lam, K. Y. Chan, and D. Y. Kang, "High-permeance metal-organic framework-based membrane adsorber for the removal of dye molecules in aqueous phase," *Environ. Sci. Nano*, 2017.

[11] V. H. Akbar Elsagh, Omid Moradi, AliFakhrib, Fahimeh Najafi, Reza Alizadeh, "Evaluation of the potential cationic dye removal using adsorption by graphene and carbon nanotubes as adsorbents surfaces," *Arab. J. Chem.*, pp. 30–33, 2013.

[12] C. Wu *et al.*, "Fabrication of ZIF-8 @ SiO 2 Micro / Nano Hierarchical Superhydrophobic Surface on AZ31 Magnesium Alloy with Impressive Corrosion Resistance and Abrasion Resistance," 2017.

[13] K. Tao, L. Cao, Y. Lin, C. Kong, and L. Chen, "A hollow ceramic fiber supported ZIF-8 membrane with enhanced gas separation performance prepared by hot dip-coating seeding," *J. Mater. Chem. A*, vol. 1, no. 42, pp. 13046–13049, 2013.

[14] K. C. and D. K. H.Ting, H.Chi, C.H.Lam, "High Permeance Metal Organic Framework Based Membrane Adsorber for Removal of Dye molecules in Aqueous Phase," *Environ. Sci.*, 2017.

[15] S. Habibi and A. Nematollahzadeh, "Enhanced water flux through ultrafiltration polysulfone membrane via addition-removal of silica nano-particles: Synthesis and characterization," *J. Appl. Polym. Sci.*, vol. 133, no. 25, pp. 1–9, 2016.

[16] J. Gu, C. Ren, X. Zong, C. Chen, and L. Winnubst, "Preparation of alumina membranes comprising a thin separation layer and a support with straight open pores for water desalination," *Ceram. Int.*, pp. 1–8, 2016.

[17] N. C. Corda and M. S. Kini, "A Review on Adsorption of Cationic Dyes using Activated Carbon," *MATEC Web Conf.*, vol. 144, p. 02022, 2018.

[18] J. Jiunn, J. Kang, E. Poh, and B. Seng, "Synthesis and size control of zeolitic imidazolate framework-8 (ZIF-8): From the perspective of reaction kinetics and thermodynamics of nucleation Synthesis and size control of zeolitic imidazolate framework-8 (ZIF-8): From the perspective of reaction kinetics and thermodynamics of nucleation," *Mater. Chem. Phys.*, vol. 216, no. September, pp. 393–401, 2018.

[19] A. Ahmed, M. Forster, J. Jin, P. Myers, and H. Zhang, "Tuning Morphology of Nanostructured ZIF-8 on Silica Microspheres and Applications in Liquid Chromatography and Dye Degradation," *ACS Appl. Mater. Interfaces*, vol. 7, no. 32, pp. 18054–18063, 2015.

[20] X. Huang *et al.*, "molybdenum disulfide nanosheets," *Nat. Commun.*, vol. 4, pp. 1444–1448, 2013.

[21] M. Yi and C. Zhang, "Advances with enhanced tribological properties as oil," *R. Soc. Chem.*, pp. 9564–9573, 2018.

[22] V. Forsberg, R. Zhang, J. Bäckström, and C. Dahlström, "Exfoliated MoS 2 in Water without Additives," pp. 1–12, 2016.

[23] A. Pandey, S. Dutta, A. Kumar, R. Raman, A. K. Kapoor, and R. Muralidhran, "Structural and optical properties of bulk MoS 2 for 2D layer growth," no. August, 2016.

[24] C. Lin, C. Tsai, F. Tseng, Y. Yu, H. Wu, and C. Hsieh, "Low-Temperature Thermally Reduced Molybdenum Disulfide as a Pt-Free Counter Electrode for Dye-Sensitized Solar Cells," *Nanoscale Res. Lett.*, no. November, pp. 0–10, 2015.

[25] C. Huang, C. Ko, L. Chen, C. Huang, K. Tung, and Y. Liao, "A simple coating method to prepare superhydrophobic layers on ceramic alumina for vacuum membrane distillation," *Sep. Purif. Technol.*, 2016.

[26] J. Duan, Y. Pan, and F. Pacheco, "High-performance polyamide thin-film- nanocomposite reverse osmosis membranes containing Hydrophobic zeolitic imidazolate framework-8," *J. Memb. Sci.*, 2015.

[27] X. Cheng, Z. Jiang, X. Cheng, H. Yang, L. Tang, and G. Liu, "Water-selective permeation in hybrid membrane incorporating multi- functional hollow ZIF-8 nanospheres," *J. Memb. Sci.*, vol. 555, no. February, pp. 146–156, 2018.

[28] S. Y. Misyura, "Contact angle and droplet evaporation on the smooth and structured wall surface in a wide range of droplet diameters," *Appl. Therm. Eng.*, vol. 113, pp. 472–480, 2017.

[29] Z. Wang, Y. Wei, Z. Xu, Y. Cao, Z. Dong, and X. Shi, "inorganic hollow fi ber nano fi ltration membrane," vol. 503, pp. 69–80, 2016.

[30] W. Lau and A. F. Ismail, "Polymeric nanofiltration membranes for textile dye wastewater treatment : Preparation , performance evaluation , transport modelling , and fouling control — a review," *DES*, vol. 245, no. 1–3, pp. 321–348, 2009.